RSC Advances

PAPER

View Article Online
View Journal | View Issue

Cite this: *RSC Adv.*, 2016, **6**, 21917

Control of resistive switching behaviors of solution-processed HfO_X-based resistive switching memory devices by n-type doping

Masoud Akbari and Jang-Sik Lee*

Received 16th January 2016
Accepted 13th February 2016

DOI: 10.1039/c6ra01369d

www.rsc.org/advances

In this study, we investigated the effect of Ni and Ta doping on resistive switching behaviors of solution-processed HfO_X-based resistive switching memory (RRAM) devices. The observations are discussed in terms of oxygen vacancies according to doping concentration. The initial resistance and forming voltages are influenced by doping concentration due to the reduction of formation energy of oxygen vacancies, whereby a higher concentration of dopant results in a lower forming voltage and initial resistance of RRAM devices. In addition, the Ni dopant has a significant effect on forming processes in HfO_X-based RRAM devices. It is observed that 10% of Ni doping can lead to forming-free behaviors. This study demonstrates the facile control of resistive switching behaviors by doping processes during the preparation of solutions and suggests that proper doping is an easy method that can lead to modulation of RRAM properties for future nonvolatile memory applications.

Introduction

With fast development of semiconductor non-volatile memory devices, conventional charge-based memories are approaching their scaling limit. Among the emerging memory devices, resistive random access memory (RRAM) is one of the most promising candidates for future applications. Despite the fact that vacuum processing methods, for instance atomic layer deposition, chemical vapor deposition and radio-frequency magnetron sputtering, are widely used in RRAM applications,[1] they have several systematic drawbacks. The ultrahigh-vacuum condition requires expensive instrumentation and high running costs, and also controlling the film composition can be limited by the choice of precursors and processing conditions.[2] Moreover, these techniques are typically slow and need high thermal budget, which can increase fabrication costs.[3] Thus, developing a simple and cost-effective processing method is crucially essential for further progress toward large-scale manufacture of electronic devices.

Recently, numerous studies have been carried out on development of solution processing for thin film electronics.[4–8] Solution-based processes such as spin coating, dip-coating, and ink-jet printing have gained much attention due to simplicity, cost effectiveness and the capability of large area deposition.[9] Moreover, owing to compatibility with flexible substrates and also printability, this method can be utilized effectively in modern electronic devices.[10] Accordingly, many research groups applied solution processing for RRAM applications.[11–13]

Among different transition metal oxides, HfO_X has shown good resistive switching behavior such as fast switching speed, low power consumption and multi-level data storage.[14] It is generally accepted that resistive switching mechanism in transition metal oxides is usually formation and rupture of conductive filaments formed from oxygen vacancies (V_O).[15] Therefore, controlling concentration of V_O in the switching layer can lead to modify the electrical properties. Doping is one of the effective methods to improve resistive switching characteristics of RRAM devices.[12,16]

Although solution processed HfO_X-based devices have been studied,[17,18] the experimental investigation of doping in such devices is not addressed. Several research groups have studied the effect of doping on resistive switching properties of HfO_X fabricated through vacuum-based processes.[19–21] According to the theoretical calculations, V_O formation energy decreases close to the dopant site. The magnitude of reduction in formation energy depends upon the valence electron number.[22,23] Therefore, it is possible to modulate V_O concentration in HfO_X by proper doping.

In this study, we investigated the effect of Ta and Ni on resistive switching behavior of solution processed HfO_X RRAM devices. Initial forming process was significantly changed by doping, whereby Ni doping can bring about forming free resistive switching. Reduction of V_O formation energy by doping results in increase of V_O concentration and, consequently, change of forming voltage.

Department of Materials Science and Engineering, Pohang University of Science and Technology (POSTECH), Pohang 790-784, Korea. E-mail: jangsik@postech.ac.kr

Experimental

Devices were fabricated according to the process flow shown in Fig. 1(a). Ti adhesion layer (10 nm) and subsequent Pt bottom electrode (100 nm) were deposited on SiO_2/Si substrate using an electron beam evaporator. In preparation of HfO_X solution, hafnium(IV) chloride 98% was used as the main precursor and 2-methoxyethanol as the solvent. Nickel(II) chloride hexahydrate and tantalum(V) chloride were used as dopant precursors. The doping concentration was 5, 10 or 15 cation atomic percent (at%), while the total solute concentration maintained 0.2 M. The precursors and the solvent were mixed and stirred in N_2 ambient for 12 hours at room temperature. Then the solution was filtered through the 0.2 μm syringe filter to separate impurities and undissolved particles. The undoped and doped HfO_X films were spin coated on the above-mentioned Pt/Ti/SiO_2/Si substrate in N_2 ambient at the rotating speed of 500 rpm for 5 s, and subsequently at 3000 rpm for 25 s. The spin coated films were dried at 130 °C for 10 min and then annealed at 300 °C for 1 hour in air ambient. Finally, circular 100 nm-thick Al top electrodes with diameter of 50 μm were deposited on top of the thin film by e-beam evaporation through a metal shadow mask. The final device structure is shown schematically in Fig. 1(b). Electrical properties were measured using a KEITHLEY 4200-SCS Semiconductor Characterization System. During electrical characterization, the bottom electrode was grounded and voltage was applied to the top electrode.

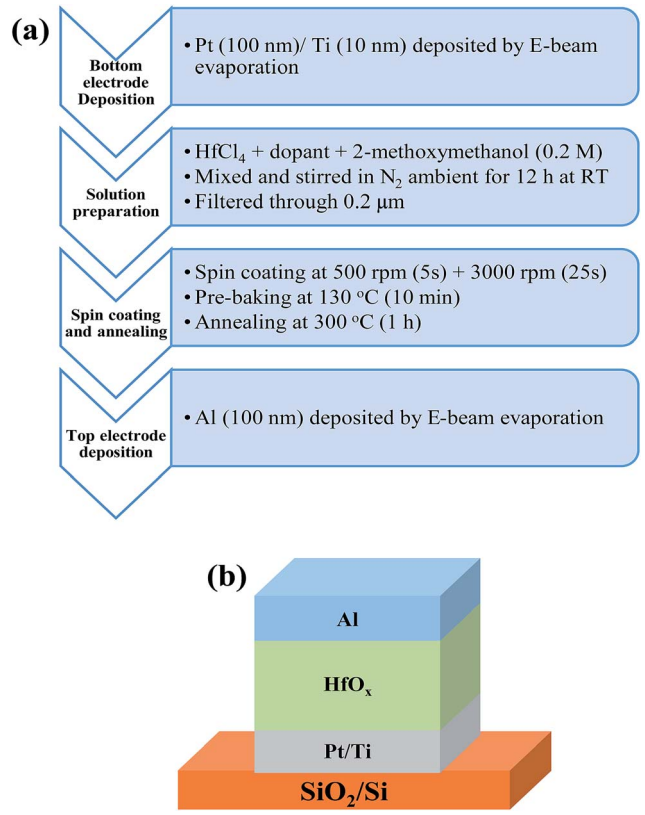

Fig. 1 (a) Process flow of RRAM device fabrication. (b) Schematic structure of Al/HfO_X/Pt RRAM devices.

Results and discussion

Fig. 2(a) shows the resistance of initial state (R_i) of devices according to the dopant concentration. The resistance is calculated by reading current at 0.5 V. The undoped device is very insulating at initial state and has the highest R_i ($\sim 10^{10}$). Doping reduces R_i, whereby higher concentration of dopant causes higher reduction of R_i. Moreover, the effect of Ni doping on R_i is more significant than Ta doping, *i.e.* in Ni doped sample R_i decreases drastically while in Ta doped sample, reduction is moderate.

The origin of the difference in R_i refers to the density of defects, *i.e.* concentration of V_O.[24] First principle calculations indicate that metal doping in HfO_X leads to decrease of V_O formation energy next to the dopant.[22,23] This reduction in formation energy is related to the valence electron number. In other words, the larger difference between dopant and Hf valence electron number, the larger reduction in V_O formation energy. Ni and Ta are both N-type dopant and their valence electron numbers are 10 and 5, respectively. Thus, Ni dopant will reduce V_O formation energy more than Ta dopant. It is expected that in Ni doped sample, density of V_O might be higher

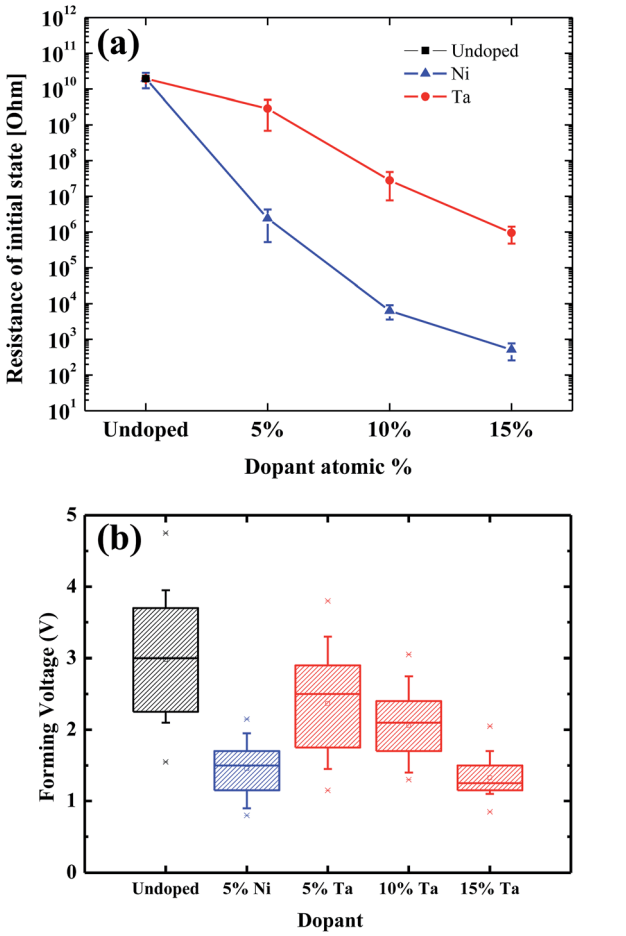

Fig. 2 (a) Resistance of initial state according to dopant concentration. (b) Statistical distribution of forming voltage in undoped and doped samples.

than Ta doped sample with same concentration of dopants and, as a result, Ni doped sample has lower R_i.

It is well known that in some pristine RRAM devices formation of the first conductive filament requires an additional forming process. This process imposes extra time and power consumption; therefore, in industrial applications it is favorable to eliminate this step. In forming process, a sufficiently large voltage is initially applied to the MIM structure. Under the high electric field, oxygen ions migrate toward the anode and an electrically conductive path (filament) from V_O will be generated along the dielectric layer. This phenomenon is regarded as a nondestructive breakdown.[26,27]

Due to effect of doping on concentration of defects, forming voltages (V_f) in the undoped and doped devices might be different. Fig. 2(b) shows the statistical distribution of V_f in undoped and doped samples. In the undoped devices, approximately 2–4 V electroforming voltage should be applied to trigger resistive switching. Since undoped HfO_x is initially very insulating V_f is relatively high.

By adding 5% Ni, V_f significantly reduced to ~1.5 V. Interestingly, the device with 10% Ni doping is forming free, *i.e.* no forming process is initially required to form the filament. Moreover, the device with 15% Ni is initially at LRS level, where resistive switching cycles should start from negative voltage sweeping. The observed behavior is closely related to the effect of Ni dopants on V_O formation energy. Since Ni dopants drastically increase the V_O concentration, a lower electric field is needed to form the filament. By increasing Ni concentration to 10%, V_O concentration would be high enough that the filament can form without forming process. When concentration of Ni dopant increases to 15%, the film may contain a large amount of V_O, leading to low initial resistance.[28]

Similar analysis can corroborate the reduction of V_f through Ta doping. Increasing the concentration of Ta dopant, results in reduction of V_f as well, which is caused by increase of V_O concentration. Since Ta dopant has lower effect on V_O formation energy compared to Ni dopant, reduction of V_f is not tremendous. Although Ta doping can decrease V_f, forming free resistive switching is not achieved.

Fig. 3(a) depicts the typical *I–V* curves of undoped device including the first initial forming process. The device shows bipolar resistive switching, *i.e.* it switches from HRS to LRS during positive voltage sweeping and returns to HRS when negative voltage is applied. A current compliance of 1 mA is imposed during positive voltage sweeping to prevent the device from hard breakdown. Formation of conductive filament from V_O is widely recognized as the switching mechanism in simple transition metal oxides. The device initially has a low concentration of V_O, so forming process is needed to generate oxygen vacancies. During forming process, large amounts of defects are generated and propagate toward the top electrode. When the filament contacts the top electrode, device switches to LRS. When negative voltage is applied oxygen ions, which have been stored at the interface of Al/HfO_X, turn back and recombine with V_O sites. Consequently, the filament will partially dissolve and device switches back to HRS.[15,29] The facts that current level of HRS is higher than of initial state (Fig. 2(a)), and set voltage is

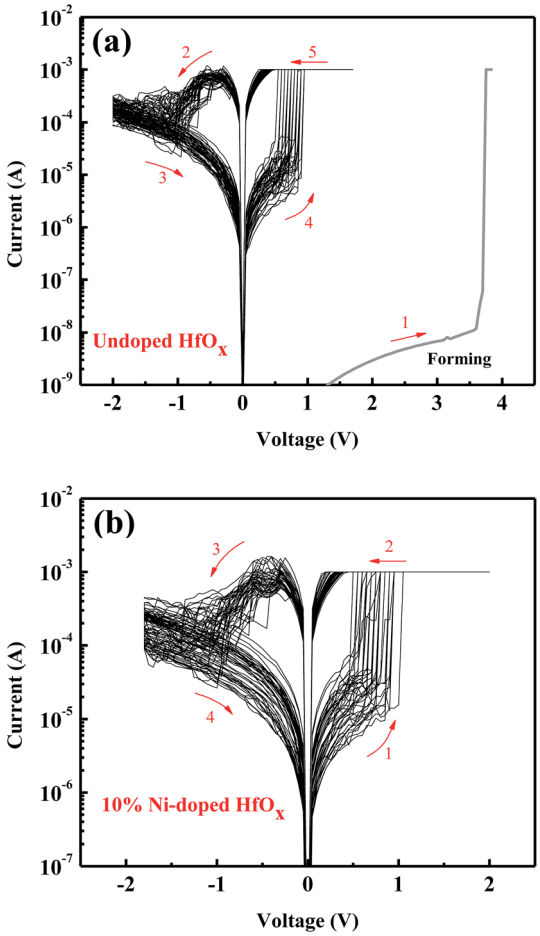

Fig. 3 Typical *I–V* curves of (a) undoped HfO_X devices including the first initial forming process and (b) 10% Ni-doped HfO_X devices.

lower than V_f reveal that filament dissociates partially in reset process.

Typical *I–V* curves of 10% Ni-doped device is shown in Fig. 3(b). No forming process was needed to trigger resistive switching cycles. *I–V* curves are generally similar to the undoped device. In other words, reset is gradual and no sharp set/reset is observed. It suggests that metal dopants do not contribute to form the metallic filament and the device is not a conductive bridging RAM. Thus, V_O filamentary switching mechanism

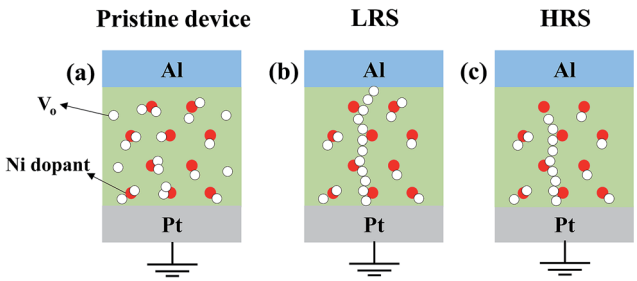

Fig. 4 Schematic illustration of resistive switching mechanism of 10% Ni-doped HfO_X devices for (a) initial state, (b) low resistance state (LRS), and (c) high resistance state (HRS); V_O denotes oxygen vacancy.

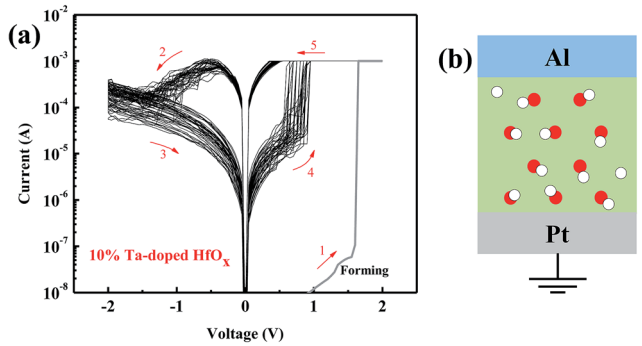

Fig. 5 (a) Typical *I–V* curves including initial forming process and (b) schematic illustration of initial state of 10% Ta-doped HfO_X devices.

might support the observed resistive switching behavior. Fig. 4 is the schematic explanation of switching in 10% Ni-doped device. In the pristine device (Fig. 4(a)), V_O clusters are formed and scattered near the dopant as a result of reduction of formation energy.[24,25] Since V_O concentration is initially large, no high electric field is needed to generate more V_O. Application of positive voltage, which is equal to the set process, causes redistribution of V_O and formation of conductive filament (Fig. 4(b)), and negative voltage sweeping results in dissociation of filament (Fig. 4(c)).

Typical *I–V* curves of 10% Ta-doped device is shown in Fig. 5(a). Compared to the undoped device, R_i and V_f decreased as a result of formation of V_O next to the Ta dopants. However, the effect of Ta doping is not as significant as Ni doping. This may be due to the fact that V_O concentration is lower in Ta-doped HfO_X than Ni-doped devices at the same dopant concentration (Fig. 5(b)).

Fig. 6(a) illustrates the variation of HRS and LRS levels of undoped and 10%-doped RRAM devices. There is a slight deterioration of uniformity in HRS after doping. This may be related to V_O concentration. In case of LRS all devices showed very small range of resistance level distribution. The relation between resistance states/distribution and doping concentration will be explored in detail based on the investigation of bonding nature and microstructural analyses in the near future. Fig. 6(b) shows the variation of set voltages of devices according to doping. The range of variation of set voltages is found to be small and no significant effect of doping on set voltages can be observed. The quality and thickness of solution-processed films can affect the electrical properties of memory devices. Further study is under way to investigate the effects of process parameters on microstructures, dimensions, and electrical properties of solution-processed memory devices.

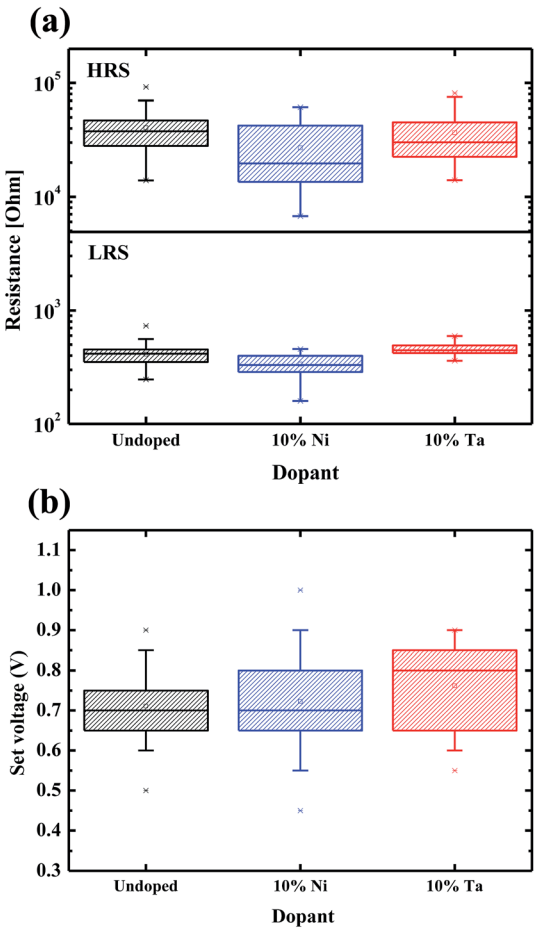

Fig. 6 Statistical distribution of (a) HRS/LRS levels and (b) set voltages of undoped and 10% doped HfO_X devices.

Conclusions

In conclusion, we investigated the effect of Ta and Ni doping on resistive switching behavior of solution processed HfO_X RRAM devices. Due to increase of V_O concentration, R_i and V_f of devices reduced by doping. It is found that effect of Ni is more significant than Ta due to the difference in valence number, resulting in difference in V_O concentration. Forming free behavior, which is strongly favorable for industrial applications, can be achieved by 10% Ni doping without any severe degradation of electrical properties. This work is based on solution processes and doping can be done facilely during HfO_X solution preparation. Therefore, this study has a great potential to be used for fabrication of RRAM devices with controlled electrical properties at low cost.

Acknowledgements

This work was supported by the Future Semiconductor Device Technology Development Program (10045226) funded by the Ministry of Trade, Industry and Energy (MOTIE), and Korea Semiconductor Research Consortium (KSRC). This work was also supported by National Research Foundation of Korea (NRF-2015R1A2A1A15055918). In addition, this work was partially supported by Brain Korea 21 PLUS project (Center for Creative Industrial Materials).

Notes and references

1 F. Pan, S. Gao, C. Chen, C. Song and F. Zeng, *Mater. Sci. Eng., R*, 2014, **83**, 1–59.

2 Y. Aoki, T. Kunitake and A. Nakao, *Chem. Mater.*, 2005, **17**, 450–458.
3 K.-H. Jang, J.-H. Park, S.-M. Oh, I. Hwang and W.-J. Cho, *Jpn. J. Appl. Phys.*, 2014, **53**, 08NE03.
4 D. B. Mitzi, *J. Mater. Chem.*, 2004, **14**, 2355–2365.
5 M.-G. Kim, M. G. Kanatzidis, A. Facchetti and T. J. Marks, *Nat. Mater.*, 2011, **10**, 382–388.
6 C. Avis and J. Jang, *J. Mater. Chem.*, 2011, **21**, 10649–10652.
7 X. Li, M. Rui, J. Song, Z. Shen and H. Zeng, *Adv. Funct. Mater.*, 2015, **25**, 4929–4947.
8 J. Song and H. Zeng, *Angew. Chem., Int. Ed.*, 2015, **54**, 9760–9774.
9 J.-B. Seon, S. Lee, J. M. Kim and H.-D. Jeong, *Chem. Mater.*, 2009, **21**, 604–611.
10 Y.-g. Ha, J. D. Emery, M. J. Bedzyk, H. Usta, A. Facchetti and T. J. Marks, *J. Am. Chem. Soc.*, 2011, **133**, 10239–10250.
11 W. Hu, L. Zou, X. Chen, N. Qin, S. Li and D. Bao, *ACS Appl. Mater. Interfaces*, 2014, **6**, 5012–5017.
12 M. S. Lee, S. Choi, C.-H. An and H. Kim, *Appl. Phys. Lett.*, 2012, **100**, 143504.
13 B. Zeng, D. Xu, M. Tang, Y. Xiao, Y. Zhou, R. Xiong, Z. Li and Y. Zhou, *J. Appl. Phys.*, 2014, **116**, 124514.
14 L. Zhao, H.-Y. Chen, S.-C. Wu, Z. Jiang, S. Yu, T.-H. Hou, H.-S. Philip Wong and Y. Nishi, *Nanoscale*, 2014, **6**, 5698–5702.
15 H.-S. Wong, H.-Y. Lee, S. Yu, Y.-S. Chen, Y. Wu, P.-S. Chen, B. Lee, F. T. Chen and M.-J. Tsai, *Proc. IEEE*, 2012, **100**, 1951–1970.
16 B. Zeng, D. Xu, Z. Tang, Y. Xiao, Y. Zhou, R. Xiong, M. Tang, Z. Li and Y. Zhou, *ECS Solid State Lett.*, 2014, **3**, Q59–Q62.
17 A. Ramadoss, K. Krishnamoorthy and S. J. Kim, *Appl. Phys. Express*, 2012, **5**, 085803.
18 K.-H. Jang, S.-M. Oh, H.-M. An and W.-J. Cho, *Curr. Appl. Phys.*, 2014, **14**, 462–466.
19 H. Zhang, L. Liu, B. Gao, Y. Qiu, X. Liu, J. Lu, R. Han, J. Kang and B. Yu, *Appl. Phys. Lett.*, 2011, **98**, 042105.
20 C.-S. Peng, W.-Y. Chang, Y.-H. Lee, M.-H. Lin, F. Chen and M.-J. Tsai, *Electrochem. Solid-State Lett.*, 2012, **15**, H88–H90.
21 H. Xie, Q. Liu, Y. Li, H. Lv, M. Wang, X. Liu, H. Sun, X. Yang, S. Long and S. Liu, *Semicond. Sci. Technol.*, 2012, **27**, 125008.
22 B. Gao, H. Zhang, S. Yu, B. Sun, L. Liu, X. Liu, Y. Wang, R. Han, J. Kang and B. Yu, in *VLSI Technology, 2009 Symposium on, IEEE*, 2009, pp. 30–31.
23 L. Zhao, S.-W. Ryu, A. Hazeghi, D. Duncan, B. Magyari-Kope and Y. Nishi, in *VLSI Technology (VLSIT), 2013 Symposium on, IEEE*, 2013, pp. T106–T107.
24 B. Gao, B. Chen, F. Zhang, L. Liu, X. Liu, J. Kang, H. Yu and B. Yu, *IEEE Trans. Electron Devices*, 2013, **60**, 1379–1383.
25 Z. Fang, H. Y. Yu, X. Li, N. Singh, G. Q. Lo and D. L. Kwong, *IEEE Electron Device Lett.*, 2011, **32**, 566–568.
26 V. Rana and R. Waser, in *Memristors and Memristive Systems*, Springer, 2014, pp. 223–251.
27 K. M. Kim, D. S. Jeong and C. S. Hwang, *Nanotechnology*, 2011, **22**, 254002.
28 X. Cao, X. Li, X. Gao, W. Yu, X. Liu, Y. Zhang, L. Chen and X. Cheng, *J. Appl. Phys.*, 2009, **106**, 073723.
29 R. Waser, R. Dittmann, G. Staikov and K. Szot, *Adv. Mater.*, 2009, **21**, 2632–2663.